

# The signature at the Tevatron for the light doubly charged Higgsino of the supersymmetric left-right model

B. Dutta<sup>1</sup>, R. N. Mohapatra<sup>2</sup> and D. J. Muller<sup>3</sup>

<sup>1</sup> *Department of Physics, Texas A&M University, College Station, TX 77840*

<sup>2</sup> *Department of Physics, University of Maryland, College Park, MD-20742*

<sup>3</sup> *Department of Physics, Oklahoma State University, Stillwater, OK 74078*

(October, 1998)

## Abstract

We analyze the signal at the Tevatron for the doubly charged Higgs superfield of supersymmetric left-right models with gauge mediated supersymmetry breaking. Due to the presence of a new coupling, the lighter stau is usually less massive than the lightest neutralino and is frequently the NLSP. The fermionic part of the doubly charged Higgs field decays dominantly into two  $\tau$  leptons plus missing energy (gravitino). We find that the inclusive two  $\tau$ -jets and three  $\tau$ -jets plus missing energy signatures could be observable at Run II of the Tevatron. We also find that the distribution in angle between the two highest  $E_T$   $\tau$ -jets when they come from same sign  $\tau$  leptons can be used to distinguish this model from the others.

## I. INTRODUCTION

Due to its many attractive features, supersymmetry (SUSY) has become a primary focus of experimental investigations. Most of the experimental searches for SUSY so far have been performed in the context of the Minimal Supersymmetric Standard Model (MSSM) [1]. It is important, however, to determine what the signatures are for SUSY models beyond the MSSM. In this work we consider SUSY left-right (LR) models with gauge mediated supersymmetry breaking (GMSB).

Supersymmetric left-right models (SUSYLR) where the  $SU(2)_R$  gauge symmetry is broken by triplet Higgs fields  $\Delta^c$  with  $B - L = 2$  have many attractive features: 1) they imply automatic conservation of baryon and lepton number [2]; 2) they provide a natural solution to the strong and weak CP problems of the MSSM [3]; 3) they yield a natural embedding of the see-saw mechanism for small neutrino masses [4] where the right-handed triplet field ( $\Delta^c$ ) that breaks the  $SU(2)_R$  symmetry also gives heavy mass to the right-handed Majorana neutrino needed for implementing the see-saw mechanism.

Recently it has been shown that the doubly charged components of the triplet Higgs fields are massless unless there are some higher dimensional operators (HDO) [5–8]. This is independent of how supersymmetry breaking is transmitted to the visible sector (*i.e.*, whether it is gravity mediated or it is gauge mediated) and also of whether the hidden sector supersymmetry breaking scale is above or below the  $W_R$  scale. In the presence of HDO's, they acquire masses of order  $\sim v_R^2/M_{\text{Pl}}$ . Since the measurement of the Z-width at LEP and SLC implies that such particles must have a mass of at least 45 GeV, this puts a lower limit on the  $W_R$  scale of about  $10^{10}$  GeV or so. For  $W_R$  near this lower limit, the masses of the doubly charged particles are in the 100 GeV range. The rest of the particle spectrum below the  $W_R$  scale can be the same as that of the MSSM with a massive neutrino or it can have an extra pair of Higgs doublets in the 10 TeV range depending on the structure of the model.

The ordering of the sparticles masses in the SUSYLR model makes the SUSY signature distinctive from other SUSY models. Of primary importance to the signal is the identity of the sparticle which is the next to lightest SUSY particle (NLSP). Here the NLSP can be the lightest neutralino, the lighter stau, or the light doubly charged Higgsino (which we henceforth call the deltino). Mass spectra for this type of model have been studied previously [9]. It was found that one of the Higgs fields has a coupling with the third generation charged leptons which reduces the third generation charged slepton masses. Because of this, in SUSYLR models with GMSB the lighter stau is predominantly the NLSP whenever the deltino is too massive to play that role. As a result, the decay chains of the SUSY particles typically lead to the lighter stau. The  $\tilde{\tau}_1$  then decays into a  $\tau$  lepton and a gravitino ( $\tilde{G}$ ) which escapes the detector undetected (leading to missing energy). Since the gravitino mass is on the order of eV, the emitted  $\tau$  will have high  $p_T$  enhancing its detection possibility. Moreover, pair production of the light doubly charged Higgsinos always produces four  $\tau$  leptons. When the  $\tilde{\tau}_1$  is the NLSP, this occurs through  $\tilde{\Delta}^{c\pm\pm} \rightarrow \tilde{\tau}_1^\pm \tau^\pm$  followed by  $\tilde{\tau}_1 \rightarrow \tau \tilde{G}$ . When the  $\tilde{\Delta}^{c\pm\pm}$  is the NLSP, this occurs through the stau mediated decay  $\tilde{\Delta}^{c\pm\pm} \rightarrow \tau^\pm \tau^\pm \tilde{G}$ . One can get a similar signal in supergravity motivated LR models with the gravitinos replaced by the lightest neutralino (its mass is greater than 33 GeV), which will constitute the missing energy.

Signals involving two or more high  $p_T$   $\tau$  leptons are also important signals for conventional GMSB models as the lighter stau is frequently the NLSP for these models as well. In the SUSYLR model, however, we find that the production of the deltino can greatly enhance the signal. In addition, since the deltino decays into like sign  $\tau$  leptons, we find that the distribution in angle between same sign  $\tau$  leptons can be used to distinguish this model from other GMSB models.

In this paper we analyze in detail the signal for SUSY production in the context of the SUSYLR model. First, we discuss the sparticle masses and the production cross sections for the major SUSY production modes:  $\chi_1^+ \chi_1^-$  production,  $\chi_1^\pm \chi_2^0$  production, slepton pair production and  $\tilde{\Delta}^{c++} \tilde{\Delta}^{c--}$  production. Next, we analyze the  $\tau$ -jet signal. We give the typical two, three and four  $\tau$ -jet inclusive production cross sections with and without standard cuts. Last, we show how the distribution in angle between the  $\tau$ -jets based on their charges can distinguish this model from other models whose signals also involve the production of  $\tau$  leptons.

## II. SPARTICLE MASSES AND PRODUCTION

Since the observed signal depends on the masses of the sparticles, we first begin by describing the model and the corresponding mass spectrum. The particle content of this model above the LR scale includes  $\phi(2, 2, 0)$ ,  $\Delta(3, 1, 2)$ ,  $\bar{\Delta}(3, 1, -2)$ ,  $\Delta^c(1, 3, -2)$ ,  $\bar{\Delta}^c(1, 3, -2)$  and a singlet where the numbers in the parentheses refer to their transformation properties under  $SU(2)_L \times SU(2)_R \times U(1)_{B-L}$ . The LR symmetric superpotential for this theory is

$$\begin{aligned}
W = & \mathbf{h}_q^{(i)} Q^T \tau_2 \Phi_i \tau_2 Q^c + \mathbf{h}_l^{(i)} L^T \tau_2 \Phi_i \tau_2 L^c \\
& + i(\mathbf{f} L^T \tau_2 \Delta L + \mathbf{f}_c L^{cT} \tau_2 \Delta^c L^c) \\
& + M_D [\text{Tr}(\Delta \bar{\Delta}) + \text{Tr}(\Delta^c \bar{\Delta}^c)] + \lambda S (\Delta \bar{\Delta} - \Delta^c \bar{\Delta}^c) + \mu_S S^2 \\
& + \mu_{ij} \text{Tr}(\tau_2 \Phi_i^T \tau_2 \Phi_j) + W_{NR}
\end{aligned} \tag{1}$$

where  $W_{NR}$  denotes nonrenormalizable terms arising from higher scale physics such as grand unified theories or Planck scale effects. Demanding that the  $F_\Delta$ ,  $F_s$  and  $F_{\Delta^c}$  terms vanish, it has been found [9] that the VEV of  $S$  becomes  $\frac{M_D}{\lambda}$ . The VEVs for the  $\Delta$  and  $\bar{\Delta}$  vanish and their masses become of the order of  $2M_D$ . Let us now see what happens to the different components of the  $\Delta^c$  fields. One linear combination of the singly charged and neutral Higgs fields pick up a mass on the order of  $v_R$ . The doubly charged Higgsinos are massless unless the nonrenormalizable terms are introduced. In the presence of  $W_{NR}$ , the doubly charged fields acquire masses of order  $v_R^2/M_{\text{Pl}}$ . This result is true when the vacuum conserves R-parity. When the vacuum breaks R-parity, the scale of the right handed  $W$ 's has an upper bound on the order of a few TeV. Therefore, in this version of the model, all particles, including the doubly charged bosons and fermions, have masses also in the few hundred GeV to TeV range. In what follows we work with the R-parity conserving version for simplicity.

After integrating out the fields at the left-right scale, we are left with the following additional part to the MSSM:

$$W = M_\Delta \Delta^{c--} \bar{\Delta}^{c++} + f_i l^c l^c \Delta^{c--} \tag{2}$$

where we have assumed that  $f$  is diagonal. The PSI experiment [10] has put an upper bound on the product of the first two generation couplings of  $f_1 f_2 < 1.2 \times 10^{-3}$ . The magnitude of  $f_3$  is unrestrained. The term  $M_\Delta$  originates from the nonrenormalizable terms.

The model considered here involves gauge mediated supersymmetry breaking. In GMSB type models the SUSY breaking is communicated to the observable sector by the SM gauge interactions [11]. We choose GMSB since the lighter stau will then have a mass that is almost always below that of the lightest neutralino. The lighter stau then decays to a  $\tau$  lepton and a gravitino. Since the gravitino is very light, the  $\tau$  lepton will typically be very energetic.

In the GMSB model, the sparticle spectrum depends on the following parameters:  $M$ ,  $\Lambda$ ,  $n$ ,  $\tan\beta$ ,  $f_3$ ,  $M_{\tilde{\Delta}}(M)$  and the sign of  $\mu$ .  $M$  is the messenger scale. The parameter  $n$  is dictated by the choice of the vector-like messenger sector. In this calculation we will assume that each flavor in the messenger sector consists of a vector like isosinglet pair of fields ( $Q + \bar{Q}$ ) and a vector like weak isodoublet pair  $L + \bar{L}$ . The definition of  $\tan\beta$  is that  $\tan\beta \equiv v_2/v_1$  where  $v_2$  is the VEV for the up-type ( $H_u$ ) Higgs doublet and  $v_1$  is the VEV for the down-type ( $H_d$ ) Higgs doublet.  $M_{\tilde{\Delta}}(M)$  is the messenger scale value for the deltino mass. The parameter  $\mu$  is the coefficient in the bilinear mixing term,  $\mu H_u H_d$ , in the superpotential. Constraints coming from  $b \rightarrow s\gamma$  strongly favor negative values for  $\mu$  [12] and, in the cases considered in this work,  $\mu$  is taken to be negative. Demanding that the EW symmetry be broken radiatively fixes the magnitude of  $\mu$  and the parameter  $B$  (from the  $B\mu H_u H_d$  term in the scalar potential) in terms of the other parameters of the theory.

The soft SUSY breaking gaugino and scalar masses at the messenger scale are given by [13]

$$\tilde{M}_i(M) = ng \left( \frac{\Lambda}{M} \right) \frac{\alpha_i(M)}{4\pi} \Lambda \quad (3)$$

and

$$\tilde{m}^2(M) = 2nf \left( \frac{\Lambda}{M} \right) \sum_{i=1}^3 k_i C_i \left( \frac{\alpha_i(M)}{4\pi} \right)^2 \Lambda^2 \quad (4)$$

where the  $\alpha_i$  are the three SM gauge couplings and  $k_i = 1, 1$  and  $3/5$  for SU(3), SU(2) and U(1), respectively. The  $C_i$  are zero for gauge singlets and are  $4/3, 3/4$  and  $(Y/2)^2$  for the fundamental representations of SU(3), SU(2) and U(1), respectively (with  $Y$  given by  $Q = I_3 + Y/2$ ).  $g(x)$  and  $f(x)$  are messenger scale threshold functions.

We calculate the SUSY mass spectrum by using the appropriate renormalization group equations [14]. We first run the Yukawa couplings (including the three new couplings  $f_{1,2,3}$ ) and the gauge couplings from the weak scale up to the messenger scale. At the messenger scale, we apply the boundary conditions given by the equations above and then use the RGEs for the soft SUSY couplings and masses in order to run down to the weak scale.

The mass spectrum here is much like that expected in minimal GMSB models. The gravitino is always the LSP. Since SUSY breaking is communicated to the visible sector by gauge interactions, the mass differences between the superparticles depend on their gauge interactions. This creates a hierarchy in mass between electroweak and strongly interacting sparticles. Eq. 3 shows that the gluino is more massive than the charginos and neutralinos, while Eq. 4 shows that the squarks are considerably more massive than the sleptons. Thus

in minimal GMSB models, the lightest neutralino and the lighter stau fight for the NLSP spot [12,15]. In this model, the deltino also joins the race to become the NLSP.

We will concentrate the analysis on those regions of the parameter space where either the lighter stau or the deltino is the NLSP. Whether or not the deltino is the NLSP depends on the mass it gets from the higher dimensional terms. If this mass is too high, then either the  $\tilde{\tau}_1$  or  $\chi_1^0$  is the NLSP. The lighter stau can be much lighter in our SUSYLR model than in conventional GMSB models due to the presence of the additional coupling  $f_3$ . Thus the lighter stau will be lighter than the  $\chi_1^0$  for a larger region of the parameter space and the  $\tilde{\tau}_1$  has a greater potential to be the NLSP in this SUSYLR model.

There are a number of potential SUSY production mechanisms here. Given the current lower bounds on the various sparticle masses and the hierarchy of sparticle masses in GMSB models, the important SUSY production mechanisms will typically include EW gaugino production. At the Tevatron, chargino pair ( $\chi_1^+ \chi_1^-$ ) production takes place through s-channel  $Z$  and  $\gamma$  exchange and  $\chi_2^0 \chi_1^\pm$  production is through s-channel  $W$  exchange. Squark exchange via the t-channel also contributes to both processes, but the contributions are expected to be negligible since the squark masses are large in GMSB models. The production of  $\chi_1^0 \chi_1^\pm$  is suppressed due to the smallness of the coupling involved.

In addition to these usual SUSY production mechanisms of the MSSM, we also have deltino pair ( $\tilde{\Delta}^{c++} \tilde{\Delta}^{c--}$ ) production. This proceeds through s-channel  $Z$  and  $\gamma$  exchange. Given that the  $\tilde{\Delta}^{c\pm\pm}$  can be relatively light, it can be a very important SUSY production mode. In fact, it frequently is the dominant mode.

The possible final state configurations at the Tevatron depend on the sparticle spectrum and on which SUSY production mode is dominant, but they will have certain aspects in common. When the  $\tilde{\tau}_1$  is the NLSP, the various possible decay modes will (usually) produce at least two  $\tau$  leptons arising from the decays of the lighter staus. In addition, there can also be large  $\cancel{E}_T$  due to the stable gravitinos and neutrinos escaping detection. When the deltino is the NLSP, the standard SUSY production modes of EW gauginos can still produce large numbers of  $\tau$ -jets if the  $\tilde{\tau}_1$  is the next to next to lightest SUSY particle (in which case the  $\tilde{\tau}_1$  is lighter than the  $\chi_1^0$ ) so that the decay chains of the sparticles will still lead to the  $\tilde{\tau}_1$ .

Pair production of the deltino leads to copious quantities of  $\tau$  leptons irrespective of what the NLSP is. This is because the deltino couples to leptons/sleptons but not to quarks/squarks. In addition, the coupling to the third generation can be much greater than the small coupling to the 1st and 2nd generations. Thus, when the  $\tilde{\tau}_1$  is the NLSP, the deltino decays via  $\tilde{\Delta}^{c\pm\pm} \rightarrow \tilde{\tau}_1^\pm \tau^\pm$  with the stau decaying via  $\tilde{\tau}_1 \rightarrow \tau \tilde{G}$ . On the other hand, when the deltino is the NLSP, it decays via the  $\tilde{\tau}$  mediated three-body decay mode  $\tilde{\Delta}^{c\pm\pm} \rightarrow \tau^\pm \tau^\pm \tilde{G}$ . Thus  $\tilde{\Delta}^{c\pm\pm}$  pair production generally results in the production of four  $\tau$  leptons (two from each deltino).

### III. TAU JET ANALYSIS

As mentioned above, SUSY production for this SUSYLR model leads to the production of copious quantities of  $\tau$  leptons.  $\tau$  leptons are typically identified at colliders by their hadronic decays to thin jets. We now give a detailed account of the possible  $\tau$ -jet signatures for SUSY production at the Tevatron in the context of the left-right GMSB model.

This analysis is performed in the context of the Main Injector (MI) and TeV33 upgrades of the Tevatron collider. The center of mass energy is taken to be  $\sqrt{s} = 2 \text{ TeV}$  and the integrated luminosity is taken to be  $2 \text{ fb}^{-1}$  for the MI upgrade and  $30 \text{ fb}^{-1}$  for the TeV33 upgrade.

In performing this analysis, the cuts employed are that final state charged leptons must have  $p_T > 10 \text{ GeV}$  and a pseudorapidity,  $\eta \equiv -\ln(\tan \frac{\theta}{2})$  where  $\theta$  is the polar angle with respect to the proton beam direction, of magnitude less than 1. Jets must have  $E_T > 10 \text{ GeV}$  and  $|\eta| < 2$ . In addition, hadronic final states within a cone size of  $\Delta R \equiv \sqrt{(\Delta\phi)^2 + (\Delta\eta)^2} = 0.4$  are merged to a single jet. Leptons within this cone radius of a jet are discounted. For a  $\tau$ -jet to be counted as such, it must have  $|\eta| < 1$ . The most energetic  $\tau$ -jet is required to have  $E_T > 20 \text{ GeV}$ . In addition, a missing transverse energy cut of  $\cancel{E}_T > 30 \text{ GeV}$  is imposed.

The signatures for SUSY production depend on the hierarchy of sparticle masses. This, in turn, depends on the values the parameters of the theory takes. The parameters considered in this analysis are  $\tan\beta = 15$ ,  $n = 2$ ,  $M/\Lambda = 3$ ,  $f_3 = 0.5$ ,  $f_2 = 0.05$  and  $f_1 = 0.05$ . We vary  $\Lambda$  from 35 to 85 TeV. For the messenger scale deltino mass, we use the values 90, 120 and 150 GeV. The masses of some of the particles of interest are given in Fig. 1 and Fig. 2. In Fig. 1 we take  $M_{\tilde{\Delta}}(M) = 90 \text{ GeV}$ , but the masses of the gauginos and sleptons (with the exception of the stau) do not vary much with the messenger scale deltino mass. Fig. 2 gives the masses of the delta boson and the deltino. The deltino mass is not very sensitive to the value of  $\Lambda$ , while the delta boson mass is highly dependent on  $\Lambda$  due to the contributions from the messenger scale loops (which give it mass along with the nonrenormalizable part). Given the substantially higher  $\Delta^c$  boson mass,  $\Delta^c$  production is not very important at the Tevatron.

There are several potential SUSY production modes here. The cross sections for the more traditional SUSY production modes are given in Fig. 3. We also have deltino pair production; the cross sections for which are tabulated in Table I. Since the deltino mass does not vary much over the values of  $\Lambda$  considered, the cross section for deltino pair production does not vary much either. This cross section is high enough for all the deltino masses considered that deltino pair production is always an important SUSY production mode. For low values of  $\Lambda$ , the EW gaugino production cross section is large with values in the hundreds of fb at  $\Lambda = 35 \text{ TeV}$ , but the cross section falls off substantially as  $\Lambda$  increases. As  $\Lambda$  increases above about 55 TeV, the cross section for EW gaugino production starts to fall below that of slepton production (in particular  $\tilde{\tau}_1^+ \tilde{\tau}_1^-$ ). In a minimal model, these sleptons modes would become the dominant SUSY production modes, but here the cross sections for slepton production fall far below that of deltino pair production. Thus the dominant SUSY production modes here are deltino pair production and, at values of  $\Lambda$  below 45 TeV or so,  $\chi_1^+ \chi_1^-$  and  $\chi_2^0 \chi_1^\pm$  production.

The decay chains depend on which sparticle is the NLSP. For the values of the parameters that are considered here, either the lighter stau or the deltino is the NLSP. Since the mass of the lighter stau increases with increasing  $\Lambda$ , the lighter stau is the NLSP for lower values of  $\Lambda$ , while the deltino is the NLSP for higher values of  $\Lambda$ . For a messenger scale deltino mass of 90 GeV, the lighter stau is the NLSP for  $\Lambda$  below about 43 TeV. For  $M_{\tilde{\Delta}}(M) = 120$  and 150 GeV, the boundaries are given by about 58 and 73 TeV, respectively. When the lighter stau is the NLSP, it decays via  $\tilde{\tau}_1 \rightarrow \tau \tilde{G}$ , and the deltino decays via the two-body mode  $\tilde{\Delta}^c \rightarrow \tilde{\tau}_1 \tau$ . Then deltino pair production leads to four  $\tau$  leptons. On the other hand,

if the deltino is the NLSP, it decays via the stau mediated three-body mode  $\tilde{\Delta}^c \rightarrow \tau\tau\tilde{G}$ . So, once again, deltino pair production again leads to the production of four  $\tau$  leptons.

The decays of the lighter selectron and smuon are given in Table II. At values of  $\Lambda$  around 35 to 40 TeV, the neutralino is lower in mass than the  $\tilde{e}_1$  and  $\tilde{\mu}_1$ . When this is the case, the main decay mode of the is  $\tilde{e}_1 \rightarrow \chi_1^0 e$  and the smuon decay is correspondingly  $\tilde{\mu}_1 \rightarrow \chi_1^0 \mu$ . When this decay is not kinematically allowed, the decay  $\tilde{e}_1 \rightarrow \tilde{\Delta}^c e$  is typically dominant if kinematically allowed. If it isn't, then the selectron decays via the three-body decays  $\tilde{e}_1^+ \rightarrow e^+ \tau^+ \tilde{\tau}_1^-$  and  $\tilde{e}_1^+ \rightarrow e^+ \tau^- \tilde{\tau}_1^+$  and/or the two-body mode  $\tilde{e}_1 \rightarrow e \tilde{G}$ .

The branching ratios for the neutralinos and lighter chargino are given in Table III. The lighter neutralino has only the three decay modes  $\chi_1^0 \rightarrow \tilde{\tau}_1 \tau$ ,  $\chi_1^0 \rightarrow \tilde{\mu}_1 \mu$  and  $\chi_1^0 \rightarrow \tilde{e}_1 e$  over the parameter space considered. Since the lighter neutralino is lighter than  $\tilde{\mu}_1$  and  $\tilde{e}_1$  for  $\Lambda < 43$  TeV, the only decay mode for  $\chi_1^0$  is  $\chi_1^0 \rightarrow \tilde{\tau}_1 \tau$ . As  $\Lambda$  increases beyond the point where the decays to the selectron and smuon become kinematically available, the branching ratios for  $\chi_1^0 \rightarrow \tilde{\mu}_1 \mu$  and  $\chi_1^0 \rightarrow \tilde{e}_1 e$  increase, but the  $\chi_1^0 \rightarrow \tilde{\tau}_1 \tau$  decay remains dominant due in large part to the fact that the mass of  $\tilde{\tau}_1$  is much lower than that of the selectron and smuon.

The chargino has only two decay modes over the allowed parameter space:  $\chi_1^\pm \rightarrow \tilde{\tau}_1 \nu_\tau$  and  $\chi_1^\pm \rightarrow \chi_1^0 W$ . At the lower values of  $\Lambda$  considered, the decay to the lighter stau is either the only decay mode available or is the dominant decay mode. For  $\Lambda$  around 40 TeV and below, the only decay mode for the lighter chargino is  $\chi_1^\pm \rightarrow \tilde{\tau}_1 \nu_\tau$ . For these values of  $\Lambda$ , the lighter stau decays via  $\tilde{\tau}_1 \rightarrow \tau \tilde{G}$  as discussed above. Thus in chargino pair production, two  $\tau$  leptons are produced. As  $\Lambda$  increases, the decay mode  $\chi_1^\pm \rightarrow \chi_1^0 W$  appears. With the subsequent decays of the lighter neutralino to the sleptons and with the deltino as the NLSP, the number of  $\tau$  leptons produced is typically four or six (in principle eight  $\tau$  leptons can be produced although this requires the rather rare three-body decays of the selectron and smuon).

The branching ratios of the second lightest neutralino are particularly sensitive to the value of  $\Lambda$ . At lower values of  $\Lambda$ , the decays to the sleptons are dominant. In particular, the decay  $\chi_2^0 \rightarrow \tilde{\tau}_1 \tau$  is dominant due to the lower mass of the  $\tilde{\tau}_1$  and the fact that the  $\chi_2^0$  is mostly wino. When the  $\tilde{\tau}_1$  is the NLSP,  $\chi_2^0 \chi_1^\pm$  production typically produces three  $\tau$ -jets. When the lighter stau isn't the NLSP and decays via  $\tilde{\tau}_1 \rightarrow \tau \tilde{\Delta}^c$ , then five  $\tau$  leptons are usually produced, although three is also common due to the decays of the  $\chi_2^0$  to the  $\tilde{\mu}_1$  and  $\tilde{e}_1$  followed by their decays to the deltino. As  $\Lambda$  increases, the decay  $\chi_2^0 \rightarrow \chi_1^0 h$  becomes dominant, but at these values of  $\Lambda$ , the cross section for EW gaugino production falls far below that of deltino pair production.

In summary, the dominant SUSY production modes at low values of  $\Lambda$  are deltino pair production and EW gaugino production. We expect four  $\tau$  leptons to be produced in deltino pair production, while EW gaugino production is typically expected to produce two to three  $\tau$  leptons. For larger values of  $\Lambda$ , the possibility exists to produce many  $\tau$  leptons in EW gaugino production, but the cross sections for such production are much smaller than that for deltino pair production. Thus four  $\tau$  leptons are generally produced at larger values of  $\Lambda$ .

We now consider the observability of these modes at Tevatron's Run II. Tables IV, V and VI give the inclusive  $\tau$ -jet production cross sections for a messenger scale deltino mass of 90, 120 and 150 GeV, respectively. We include in the figures only up to four  $\tau$ -jets as the

cross sections for more than four  $\tau$ -jets are small. Considering Table IV, we see that before cuts the production of two and three  $\tau$ -jets are dominant, but the four  $\tau$ -jet cross section is also significant at slightly over 100 fb. After the cuts are applied, however, the situation changes substantially. The one  $\tau$ -jet mode is now dominant, but the cross section for two  $\tau$ -jets is not far below and the three  $\tau$ -jets cross section is not insignificant.

We first consider the  $M_{\tilde{\Delta}}(M) = 90 \text{ GeV}$  case. We see from Table IV that for  $\Lambda = 35 \text{ TeV}$  the cross section for inclusive production of three  $\tau$ -jets is 32.3 fb. For an integrated luminosity of  $2 \text{ fb}^{-1}$  (the approximate initial value at Run II), this corresponds to about 65 events. For  $30 \text{ fb}^{-1}$ , the number of observable events is  $\sim 970$ . For  $\Lambda = 85 \text{ TeV}$ , the production cross section for three  $\tau$ -jets has gone down slightly due to the decrease in production of charginos and neutralinos. With a value of 26.7 fb, the number of expected events is about 53 and 800 for  $2 \text{ fb}^{-1}$  and  $30 \text{ fb}^{-1}$  of data, respectively. The cross section for two  $\tau$ -jets is considerably higher. For  $\Lambda = 35 \text{ TeV}$ , the  $\sigma \cdot \text{BR}$  for two  $\tau$ -jets is 125 fb which corresponds to 250 events for  $2 \text{ fb}^{-1}$  of data and 3750 events for  $30 \text{ fb}^{-1}$  of data. For  $\Lambda = 85 \text{ TeV}$ ,  $\sigma \cdot \text{BR}$  has decreased to 79 fb. This gives about 160 and 2370 events for  $2 \text{ fb}^{-1}$  and  $30 \text{ fb}^{-1}$  of data, respectively. In comparison to the GMSB model with the MSSM symmetry, the two  $\tau$ -jets and the three  $\tau$ -jets cross sections are considerably higher in this model. In the GMSB model with MSSM symmetry, the two  $\tau$ -jets cross section can be seen at RUN II, but not the three  $\tau$  jets [16].

As the mass of the deltino increases, the production rates go down and more variations appear. The inclusive  $\tau$ -jet cross sections for  $M_{\tilde{\Delta}}(M) = 120 \text{ GeV}$  are shown in Table V. Considering the inclusive three  $\tau$ -jets mode, the production cross section at  $\Lambda = 35 \text{ TeV}$  is 26 fb. This corresponds to 52 events for  $2 \text{ fb}^{-1}$  of data and 780 events for  $30 \text{ fb}^{-1}$  of data. This goes down to about 17 fb at  $\Lambda = 85 \text{ TeV}$ . This gives about 34 and 510 events for  $2 \text{ fb}^{-1}$  and  $30 \text{ fb}^{-1}$  of data, respectively. The production rate for two  $\tau$ -jets is higher. At  $\Lambda = 35 \text{ TeV}$ ,  $\sigma \cdot \text{BR} = 94 \text{ fb}$  which gives 190 and 2820 events for  $2 \text{ fb}^{-1}$  and  $30 \text{ fb}^{-1}$  of data, respectively.

#### IV. ANGULAR DISTRIBUTIONS

The excess of  $\tau$ -jets expected in this model does not constitute an unequivocal signal for this model.  $\tau$ -jets are part of the signatures for other models including the minimal GMSB model when the lighter stau is the NLSP. The question then arises as to whether there is any way to distinguish this model from the minimal GMSB model. A possible distinguishing characteristic is the distribution in angle between the two highest  $E_T$   $\tau$ -jets when they come from same sign  $\tau$ -jets.

Consider deltino pair production. The deltino tends to decay to like sign  $\tau$  leptons. This occurs directly when the deltino is the NLSP and so decays via the three-body decay  $\tilde{\Delta}^{\pm\pm} \rightarrow \tau^{\pm}\tau^{\pm}\tilde{G}$ . When the two-body decay of the deltino  $\tilde{\Delta}^{\pm\pm} \rightarrow \tilde{\tau}_1^{\pm}\tau^{\pm}$  occurs, then the second like sign  $\tau$  lepton comes from the subsequent decay of the stau. In the rest frame of the deltino, the  $\tau$  leptons are widely distributed. In the lab frame, however, the deltinios are quite energetic and have a large velocity, especially if their masses are small. As a consequence of this, the decay products of the deltino tend to be collimated in the direction in which the deltino was moving. Thus when the two most energetic  $\tau$ -jets have the same



sign in deltino pair production, the angle between them tends to be smaller than when the two most energetic  $\tau$ -jets have opposite sign charges.

Fig. 4 gives the distribution in angle between the two most energetic  $\tau$ -jets for deltino pair production. This example is for a weak scale deltino mass of about 97 GeV. We can see that the distribution in angle for like sign  $\tau$ -jets, which is given in Fig. 4(a), peaks at about  $40^\circ$ . Fig. 4(b) gives the distribution in angle between the two most energetic  $\tau$ -jets when they come from opposite sign  $\tau$  leptons. In stark contrast to the previous case, here the peak occurs at  $110^\circ$ .

The question then arises as to how these distributions look in the usual SUSY production modes. Fig. 5 shows the angular distributions for combined  $\chi_2^0 \chi_1^\pm$  and  $\chi_1^+ \chi_1^-$  production for the input parameters  $M = 100$  TeV,  $\Lambda = 45$  TeV,  $n = 1$  and  $\tan \beta = 10$ . For these values of the parameters, the weak scale  $\chi_2^0$  mass is  $\sim 100$  GeV. The distribution for same sign  $\tau$ -jets is given in Fig 5(a). We see that the peak occurs at about  $110^\circ$ . In this situation, same-sign  $\tau$ -jets do not come from  $\chi_1^+ \chi_1^-$  production. In  $\chi_2^0 \chi_1^\pm$  production, one of the same sign  $\tau$ -jets generally comes from the chargino and the other from the neutralino. We now consider the angular distribution for opposite sign  $\tau$ -jets which are given in Fig. 5(b). In  $\chi_2^0 \chi_1^\pm$  production, opposite sign  $\tau$ -jets frequently come from the neutralino, while in  $\chi_1^+ \chi_1^-$  production one of the  $\tau$ -jets comes from one of the charginos and the other  $\tau$ -jet comes from the other chargino. Since there is a strong possibility that the opposite sign  $\tau$ -jets come from the same particle ( $\chi_2^0$ ), the distribution should peak at a lower angle than for same sign  $\tau$ -jets. We see from the figure that the peak occurs at about  $85^\circ$ .

The question arises as to how much this changes as the gaugino masses are increased. Fig. 6 gives the angular distribution for a  $\chi_2^0$  mass of 150 GeV. We see that the same sign distribution still peaks at about  $110^\circ$ , while the opposite sign distribution has now shifted to a slightly higher value of about  $95^\circ$ .

The actual angular distribution between the two highest  $E_T$   $\tau$ -jets depends on which SUSY production modes are important. For certain regions of the parameter space (depending, in particular, on the values of  $\Lambda$  and the messenger scale deltino mass), deltino pair production is the only important SUSY production mode. When this is the case, the angular distributions are simply given by those for deltino pair production.

In other regions of the parameter space, EW gaugino production can be significant. We consider the angular distributions for an example given by the input parameters  $\tan \beta = 15$ ,  $n = 2$  and  $M/\Lambda = 3$ . Three values of the messenger scale deltino mass are considered: 90, 120 and 150 GeV. The angular distributions for  $M_{\tilde{\Delta}}(M) = 90$  GeV are given in Fig. 7. Since the deltino is especially light at 96 GeV, deltino pair production is the dominant SUSY production mode. Thus deltino pair production largely dictates the form of the angular distributions.

Fig. 7(a) gives the angular distribution between the two highest  $E_T$   $\tau$ -jets when they come from same sign  $\tau$  leptons. In the figure we can see the rather striking peak at around  $40^\circ$ . This is due to the same sign  $\tau$ -jets coming mostly from the decay of the same deltino. Since the deltino mass is especially light compared to the beam energy, they typically move rapidly in the lab frame. Thus their decay products tend to be more tightly collimated than in the production of the heavier particles.

Fig. 7(b) gives the angular distribution between the two highest  $E_T$   $\tau$ -jets when they come from opposite sign  $\tau$  leptons. We see from this figure that the peak occurs at about

110°. Here the  $\tau$ -jets typically come from the decay chains of different particles and so the angle between the  $\tau$ -jets is typically quite large.

The situation changes as the deltino mass gets larger. This is in part due to the fact that the deltino pair production cross section gets smaller and so production of charginos and neutralinos can have a larger impact on the distributions. In addition, a larger deltino mass means the deltininos will typically be moving slower. Thus the boost effect won't have as dramatic an effect on the deltino's decay products. The example with  $M_{\tilde{\Delta}}(M) = 120$  GeV is given in Fig. 8. We can see that the distribution for same sign  $\tau$ -jets peaks at about 70°. On the other hand, the opposite sign  $\tau$ -jet angular distribution still peaks at around 110°. Thus the angle between the  $\tau$ -jets is less striking a signature than it was before, but it is still distinctive.

The results for a messenger scale deltino mass of 150 GeV is given in Fig. 9. The peak in the distribution in angle between the two highest  $E_T$   $\tau$ -jets when they have the same sign peaks at a rather high 95°. As before, the peak in the distribution for the two highest  $E_T$   $\tau$ -jets when they have opposite sign is at 110°. Thus the distinctiveness due to the angle between the two highest  $E_T$   $\tau$ -jets is nearly lost for such a large value of the deltino mass. This is partially due to the deltino pair cross section of 92 fb being quite a bit lower than the cross section for  $\chi_1^\pm \chi_2^0$  production and  $\chi_1^+ \chi_1^-$  production. In addition, as discussed above, there is also the reduction in the boost effect as the mass of the decaying deltino increases.

## V. CONCLUSION

In conclusion, we have found that the doubly charged Higgs bosons of LR models can be potentially observable at Run II of the Tevatron through the production of  $\tau$ -jets. In a GMSB type theory, SUSYLR models typically produce large numbers of two and three  $\tau$ -jet final states. This large  $\tau$ -jet signal is also due in large part to pair production of the doubly charged Higgsino. It is also due to the relatively low mass of the lighter stau (which is frequently the NLSP) in these models, which is due to the additional coupling  $f$ . We have also shown that the distribution in angle between the two highest  $E_T$   $\tau$ -jets is different from other models which do not have this doubly charged Higgsino.

## ACKNOWLEDGMENTS

The work of R. N. M. is supported by National Science Foundation grant No. PHY-9421385 and that of D. M. by DE-FG03-98ER41076. We thank T. Kamon for valuable comments and suggestions.

## REFERENCES

- [1] For a recent review, see J. Gunion, hep-ph/9810394; H. Baer, C-H. Chen, M. Drees, F. Paige and X. Tata, hep-ph/9809223; V. Barger, C. Kao and T-J. Li, Phys. Lett. B **433**, 328 (1998).
- [2] R. N. Mohapatra, Phys. Rev. D **34**, 3457 (1986); A. Font, L. Ibanez and F. Quevedo, Phys. Lett. B **228**, 79 (1989); S. Martin, Phys. Rev. D **46**, 2769 (1992).
- [3] R. N. Mohapatra and A. Rasin, Phys. Rev. Lett. **76**, 3490 (1996); R. Kuchimanchi, Phys. Rev. Lett. **76**, 3486 (1996); R. N. Mohapatra, A. Rasin and G. Senjanović, Phys. Rev. Lett. **79**, 4744 (1997).
- [4] M. Gell-Mann, P. Ramond and R. Slansky, in *Supergravity*, ed. D. Freedman et al. (North Holland, 1979); T. Yanagida, KEK Lectures (1979); R. N. Mohapatra and G. Senjanović, Phys. Rev. Lett. **44**, 912 (1980).
- [5] R. Kuchimanchi and R. N. Mohapatra, Phys. Rev. D **48**, 4352 (1993); *ibid.* Phys. Rev. Lett. **75**, 3989 (1995).
- [6] C. S. Aulakh, A. Melfo and G. Senjanović, hep-ph/9707258; C. S. Aulakh, A. Melfo, A. Rasin and G. Senjanović, hep-ph/9712551.
- [7] Z. Chacko and R. N. Mohapatra, hep-ph/9712359.
- [8] C. S. Aulakh, K. Benakli and G. Senjanović, Phys. Rev. Lett. **79**, 2188 (1997).
- [9] B. Dutta and R. N. Mohapatra, hep-ph/9804277 (to appear in PRD).
- [10] L. Willmann *et al.*, hep-ex/9807011; K. Jungman, invited talk in PASCOS98 (1998).
- [11] M. Dine, A. Nelson, Phys. Rev. D **48**, 1277 (1993); M. Dine, A. E. Nelson, Y. Nir and Y. Shirman, Phys. Rev. D **53**, 2658 (1996); A. E. Nelson, hep-ph/9511218; M. Dine, A. E. Nelson, and Y. Shirman, Phys. Rev. D **51** (1995) 1362.
- [12] S. Dimopoulos, S. Thomas and J.D. Wells, Nucl. Phys. **B488**, 39 (1997) ; H. Baer, M. Brhlik, C.-H. Chen and X. Tata, Phys. Rev. D **55**, 4463 (1997); N. G. Deshpande, B. Dutta and S. Oh, Phys. Rev. D **56**, 519 (1997); R. Rattazzi and Uri Sarid, Nucl. Phys. **B501**, 297 (1997).
- [13] S. Martin, hep-ph/9709356, to appear in *Perspectives in Supersymmetry*, ed. G. Kane (World Scientific, 1998)
- [14] V. Barger, M. A. Berger and P. Ohmann, Phys. Rev. D **47**, 1093 (1993); *ibid.* **49**, 4908 (1994).
- [15] J. A. Bagger, K. Matchev, D. M. Pierce, R-J. Zhang, Phys. Rev. D **55**, 3188 (1997).
- [16] B. Dutta, D. J. Muller and S. Nandi, hep-ph/9807390.

FIGURES

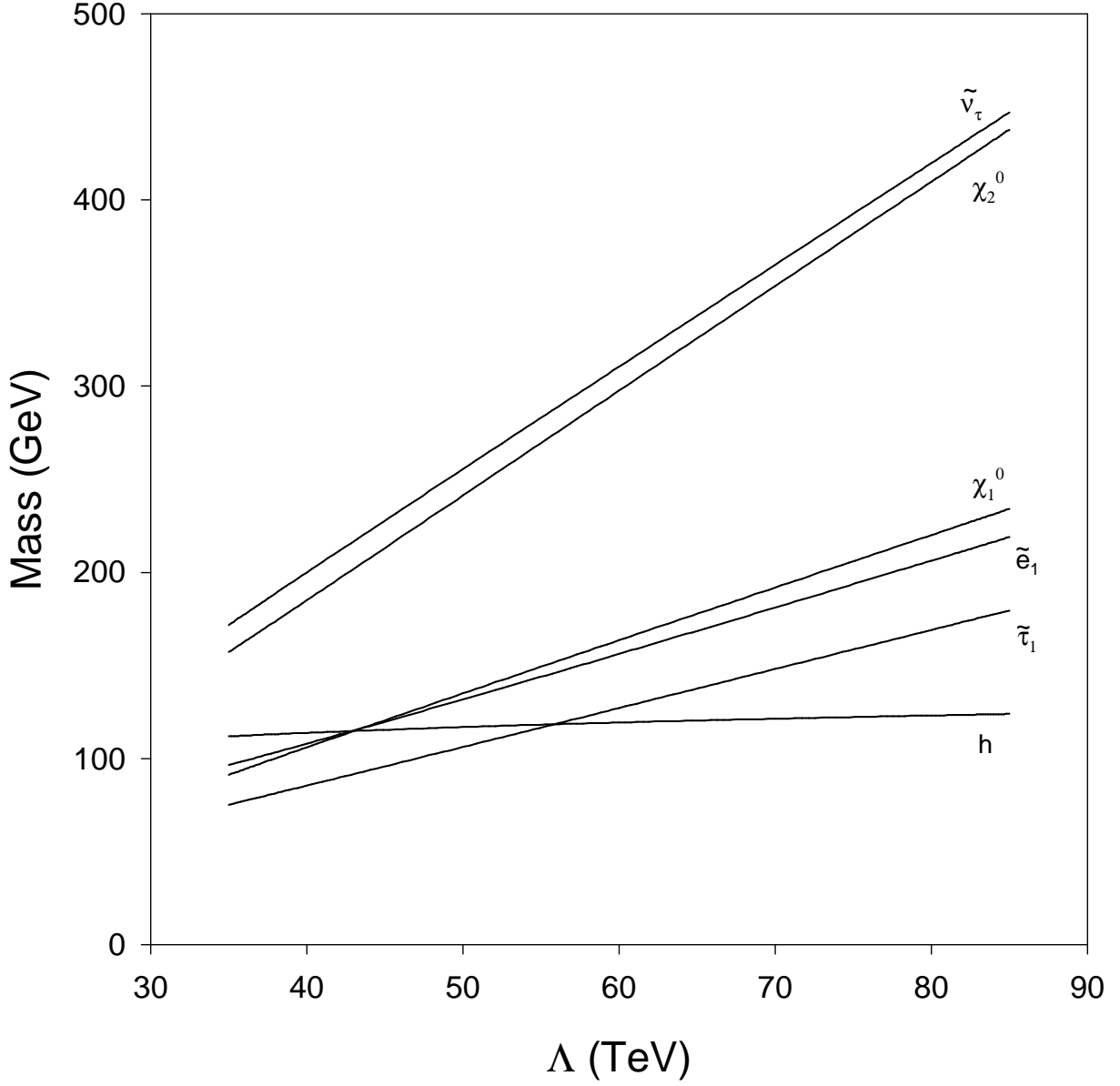


FIG. 1. Masses of the particles of interest for the input parameters  $\tan\beta = 15$ ,  $M/\Lambda = 3$ ,  $n = 2$ ,  $f_3 = 0.5$ ,  $f_2 = 0.05$ ,  $f_1 = 0.05$  and  $M_{\tilde{\Delta}}(M) = 90$  GeV.

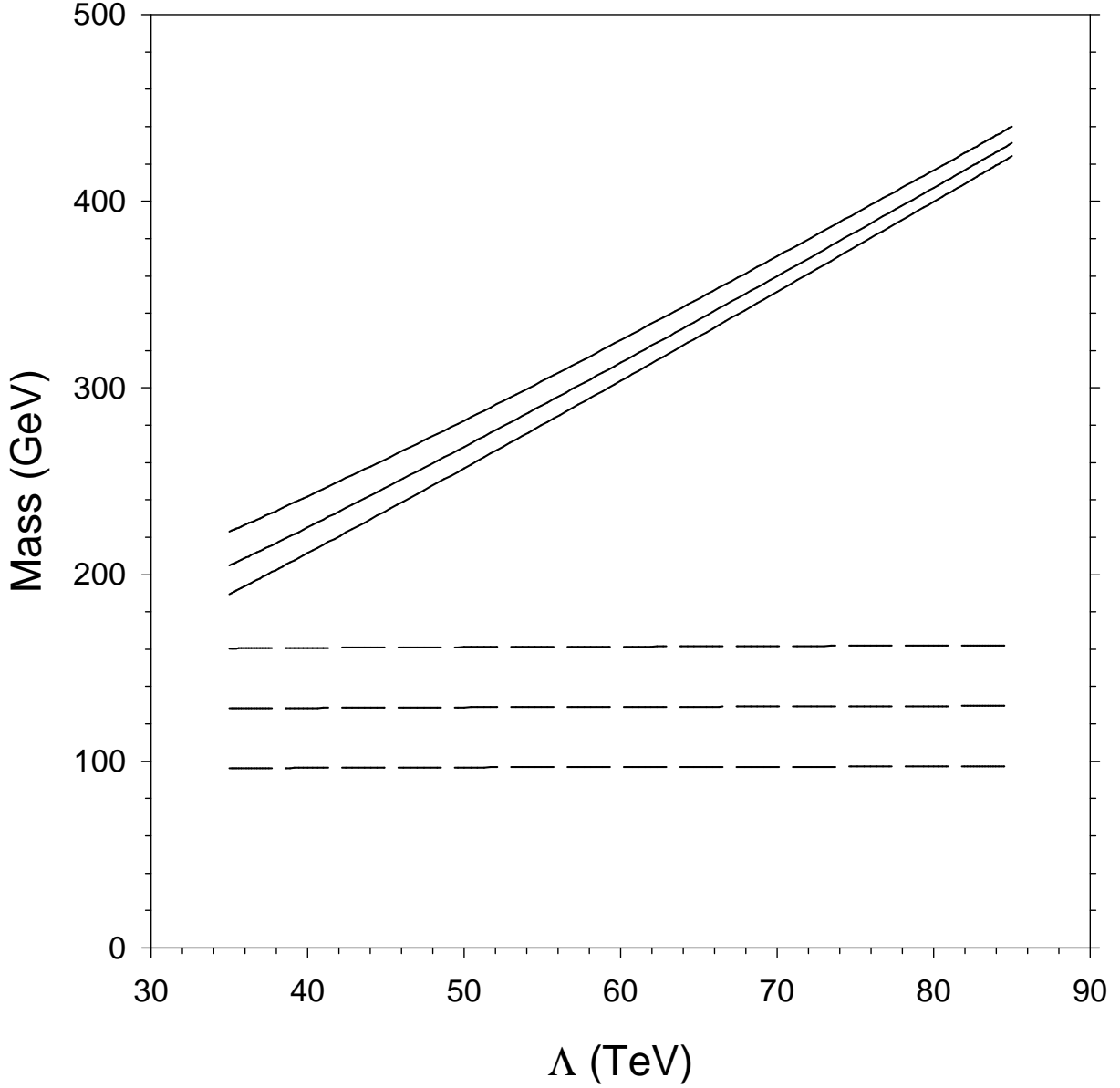


FIG. 2. Masses of the delta and deltino. The dashed lines represent the deltino, while the solid lines represent the delta boson. The parameters used are  $\tan \beta = 15$ ,  $n = 2$  and  $M/\Lambda = 3$ . From bottom to top, the lines in each set are for a messenger scale deltino mass of 90, 120 and 150 GeV.

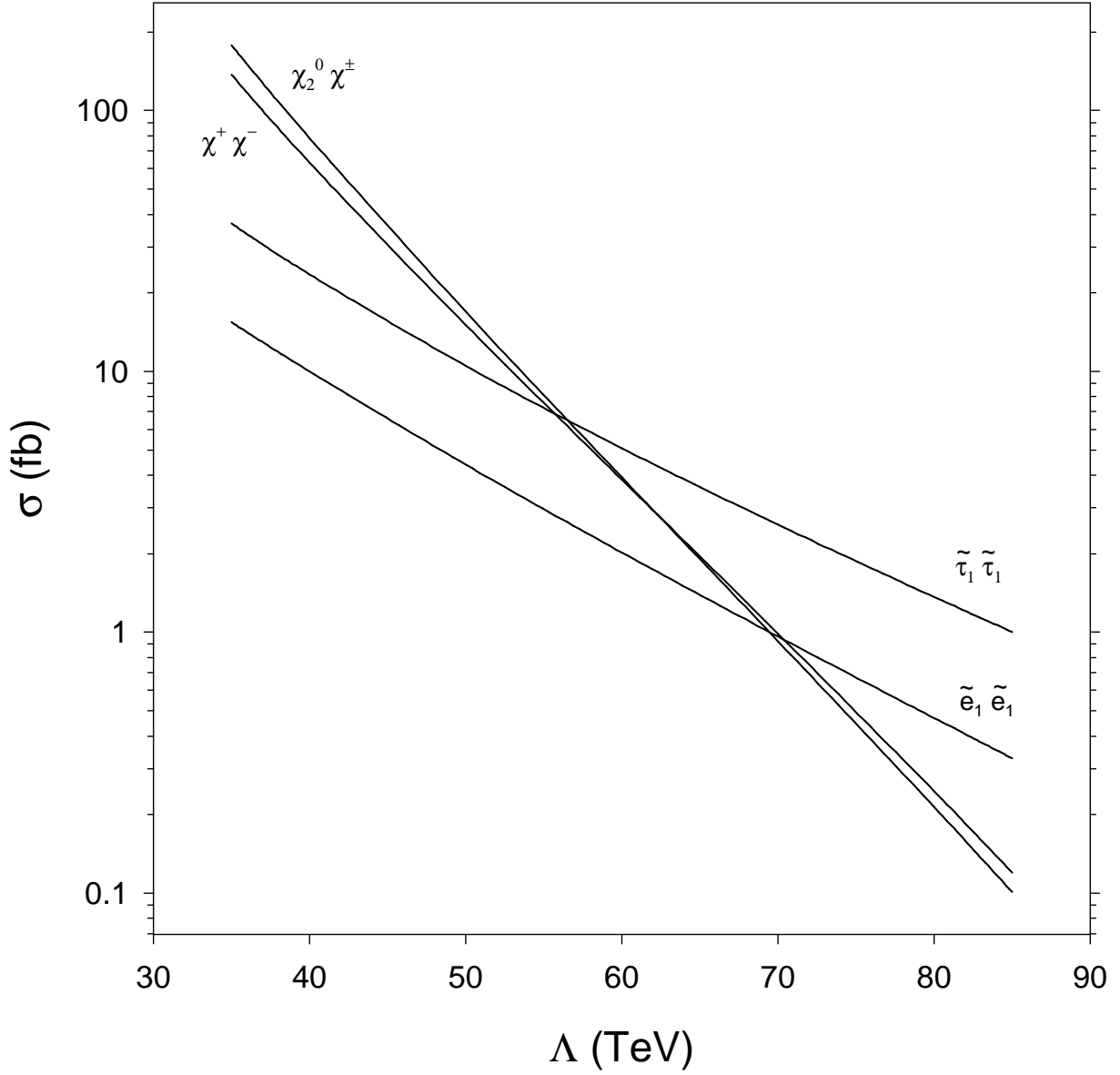


FIG. 3. Cross sections for the standard SUSY production modes for the parameters  $\tan \beta = 15$ ,  $M/\Lambda = 3$ ,  $n = 2$ ,  $f_3 = 0.5$ ,  $f_2 = 0.05$ ,  $f_1 = 0.05$  and  $M_{\tilde{\Delta}}(M) = 90$  GeV.

TABLES

TABLE I. Cross sections (in fb) for deltino pair production for various values of  $\Lambda$ . The other parameters used are  $\tan\beta = 15$ ,  $n = 2$  and  $M/\Lambda = 3$ .

$M_{\tilde{\Delta}}(M)$	$\Lambda = 35$ TeV	$\Lambda = 60$ TeV	$\Lambda = 85$ TeV
90 GeV	643.0	629.9	621.5
120 GeV	228.2	222.9	219.6
150 GeV	91.6	89.2	87.7

TABLE II. Branching ratios of the sleptons. The values of the parameters are  $\tan\beta = 15$ ,  $n = 2$  and  $M/\Lambda = 3$ .

$\Lambda$ (TeV)	35	40	50	60	70	80	85
$M_{\tilde{\Delta}}(M) = 90$ GeV							
$\tilde{e}_1 \rightarrow e\chi_1^0$	1	0.9252	-	-	-	-	-
$\tilde{e}_1 \rightarrow e\tilde{\Delta}$	-	0.0748	1	1	1	1	1
$\tilde{\tau}_1 \rightarrow \tau\tilde{G}$	1	1	-	-	-	-	-
$\tilde{\tau}_1 \rightarrow \tau\tilde{\Delta}$	-	-	1	1	1	1	1
$M_{\tilde{\Delta}}(M) = 120$ GeV							
$\tilde{e}_1 \rightarrow e\chi_1^0$	1	1	-	-	-	-	-
$\tilde{e}_1^+ \rightarrow e^+\tau^+\tilde{\tau}_1^-$	-	-	0.2065	-	-	-	-
$\tilde{e}_1^+ \rightarrow e^+\tau^-\tilde{\tau}_1^+$	-	-	0.1684	-	-	-	-
$\tilde{e}_1 \rightarrow e\tilde{\Delta}$	-	-	0.6251	1	1	1	1
$\tilde{\tau}_1 \rightarrow \tau\tilde{G}$	1	1	1	1	-	-	-
$\tilde{\tau}_1 \rightarrow \tau\tilde{\Delta}$	-	-	-	-	1	1	1
$M_{\tilde{\Delta}}(M) = 150$ GeV							
$\tilde{e}_1 \rightarrow e\chi_1^0$	1	1	-	-	-	-	-
$\tilde{e}_1^+ \rightarrow e^+\tau^+\tilde{\tau}_1^-$	-	-	0.5532	0.5643	-	-	-
$\tilde{e}_1^+ \rightarrow e^+\tau^-\tilde{\tau}_1^+$	-	-	0.4468	0.4357	-	-	-
$\tilde{e}_1 \rightarrow e\tilde{\Delta}$	-	-	-	-	1	1	1
$\tilde{\tau}_1 \rightarrow \tau\tilde{G}$	1	1	1	1	1	-	-
$\tilde{\tau}_1 \rightarrow \tau\tilde{\Delta}$	-	-	-	-	-	1	1

TABLE III. Branching ratios of some of the sparticles of interest. The values of the parameters are  $\tan\beta = 15$ ,  $n = 2$  and  $M/\Lambda = 3$ . The messenger scale deltino mass is 90 GeV, but the branching ratios of these sparticles have little dependence on the deltino mass.

$\Lambda$ (TeV)	35	40	50	60	70	80	85
$\chi_1^\pm \rightarrow \tilde{\tau}_1 \nu_\tau$	1	1	0.7153	0.5807	0.5166	0.4796	0.4663
$\chi_1^\pm \rightarrow \chi_1^0 W$	-	-	0.2847	0.4193	0.4834	0.5204	0.5337
$\chi_2^0 \rightarrow \tilde{\tau}_1 \tau$	0.6312	0.6587	0.6860	0.4034	0.3133	0.2706	0.2560
$\chi_2^0 \rightarrow \tilde{e}_1 e$	0.1844	0.1707	0.1366	0.0625	0.0386	0.0270	0.0232
$\chi_2^0 \rightarrow \tilde{\mu}_1 \mu$	0.1844	0.1707	0.1366	0.0625	0.0386	0.0270	0.0232
$\chi_2^0 \rightarrow \chi_1^0 Z$	-	-	0.0408	0.0325	0.0277	0.0252	0.0243
$\chi_2^0 \rightarrow \chi_1^0 h$	-	-	-	0.4392	0.5818	0.6501	0.6733
$\chi_1^0 \rightarrow \tilde{\tau}_1 \tau$	1	1	0.9692	0.9099	0.8723	0.8506	0.8436
$\chi_1^0 \rightarrow \tilde{e}_1 e$	-	-	0.0154	0.0451	0.0638	0.0747	0.0782
$\chi_1^0 \rightarrow \tilde{\mu}_1 \mu$	-	-	0.0154	0.0451	0.0638	0.0747	0.0782

TABLE IV. Inclusive  $\tau$ -jet production cross sections for a messenger scale deltino mass of 90 GeV. The other parameters are  $\tan\beta = 15$ ,  $n = 2$  and  $M/\Lambda = 3$ .

$\Lambda$ (TeV)	35	40	50	60	70	80	85
	$\sigma \cdot \text{BR}$ (fb)						
1 $\tau$ -jet: before cuts	198.6	132.9	73.11	71.64	70.86	70.34	70.14
after cuts	168.7	156.2	97.49	91.90	90.15	89.33	89.05
2 $\tau$ -jets: before cuts	362.6	277.3	203.6	196.7	196.3	194.8	194.2
after cuts	124.6	93.11	89.59	82.91	80.59	79.63	79.33
3 $\tau$ -jets: before cuts	306.0	273.5	253.6	244.7	240.9	238.8	238.0
after cuts	32.31	17.75	32.45	29.02	27.53	26.88	26.73
4 $\tau$ -jets: before cuts	119.4	116.9	126.42	116.5	113.1	111.6	111.1
after cuts	3.21	1.18	5.26	4.28	3.67	3.45	3.39

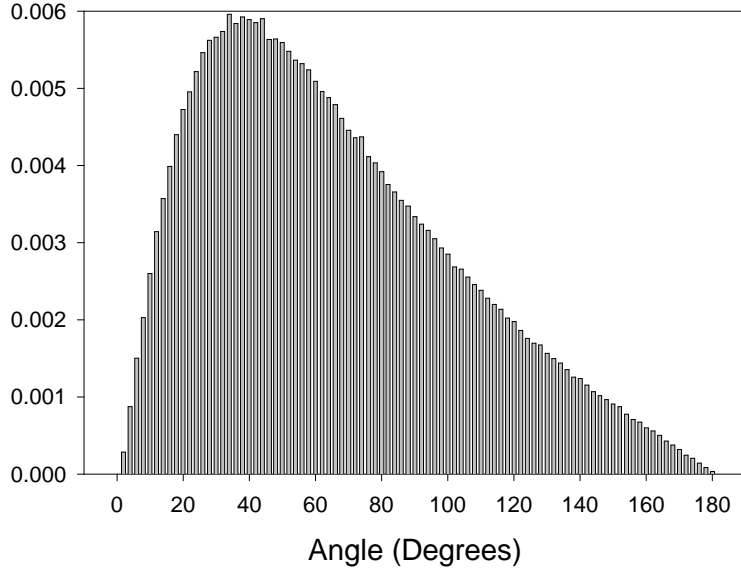


TABLE V. Inclusive  $\tau$ -jet production cross sections for a messenger scale deltino mass of 120 GeV. The other parameters are  $\tan\beta = 15$ ,  $n = 2$  and  $M/\Lambda = 3$ .

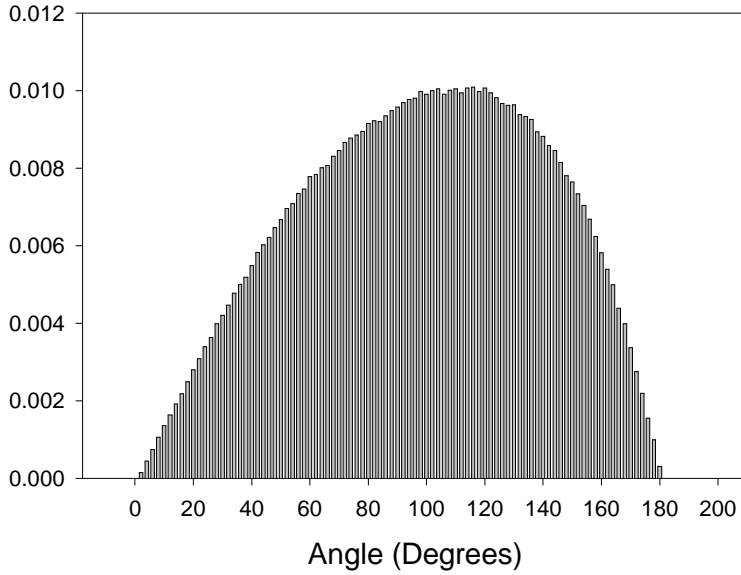
$\Lambda$ (TeV)	35	40	50	60	70	80	85
	$\sigma \cdot \text{BR}$ (fb)						
1 $\tau$ -jet: before cuts	151.5	86.21	39.60	29.72	25.30	25.00	24.90
after cuts	125.3	85.20	53.68	75.87	42.16	41.38	41.16
2 $\tau$ -jets: before cuts	232.8	148.0	90.27	75.93	70.06	69.15	68.83
after cuts	93.94	71.59	49.79	28.57	43.81	42.83	42.55
3 $\tau$ -jets: before cuts	147.6	115.9	96.70	88.92	86.55	85.16	84.71
after cuts	25.99	23.22	17.33	0.55	17.37	16.80	16.64
4 $\tau$ -jets: before cuts	46.22	44.03	42.59	40.70	40.72	39.55	39.22
after cuts	3.05	3.09	2.29	0.06	2.70	2.50	2.44

TABLE VI. Inclusive  $\tau$ -jet production cross sections for a messenger scale deltino mass of 150 GeV. The other parameters are  $\tan\beta = 15$ ,  $n = 2$  and  $M/\Lambda = 3$ .

$\Lambda$ (TeV)	35	40	50	60	70	80	85
	$\sigma \cdot \text{BR}$ (fb)						
1 $\tau$ -jet: before cuts	136.2	70.92	24.42	14.61	11.80	10.07	10.00
after cuts	105.3	65.54	32.12	22.59	23.50	19.28	18.97
2 $\tau$ -jets: before cuts	190.3	105.7	48.32	34.22	30.01	27.89	27.67
after cuts	72.17	50.55	31.35	24.29	18.99	21.75	21.46
3 $\tau$ -jets: before cuts	95.31	63.85	45.21	37.72	35.14	34.47	34.14
after cuts	17.23	14.64	12.24	10.14	5.53	9.32	9.24
4 $\tau$ -jets: before cuts	21.81	19.75	18.58	17.00	16.16	16.23	15.96
after cuts	1.73	1.81	1.89	1.67	0.59	1.46	1.47

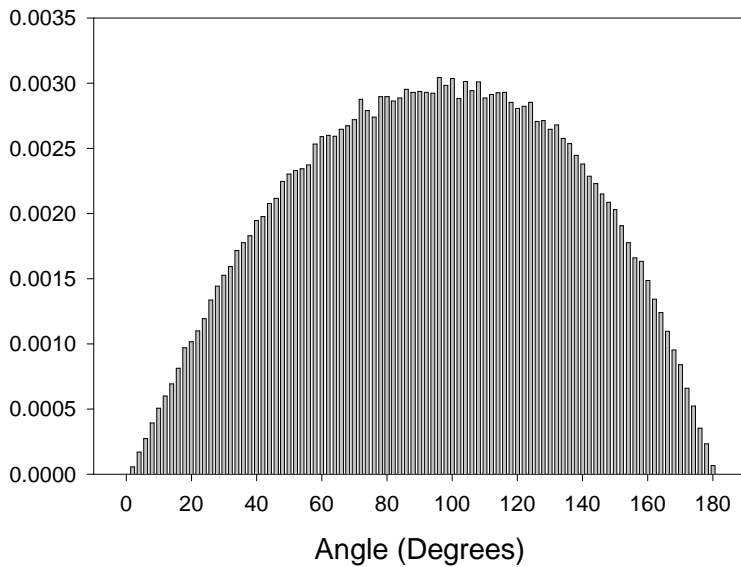


(a)

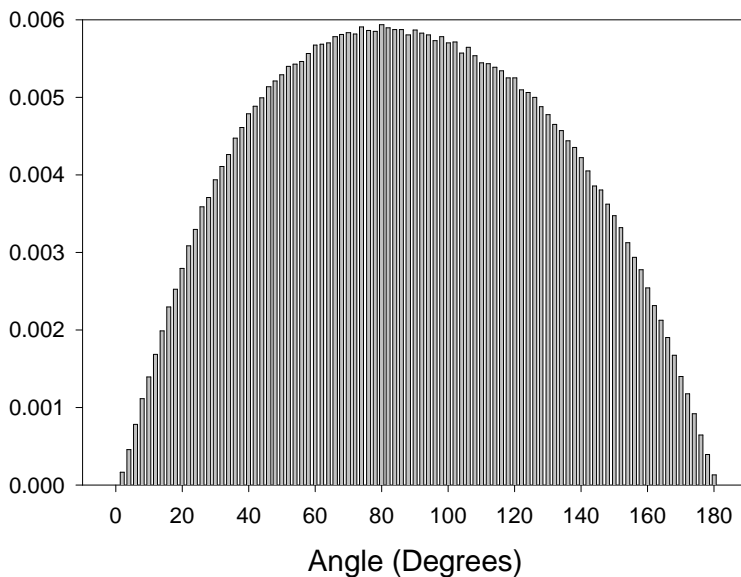


(b)

FIG. 4. Angular distribution between the two most energetic  $\tau$ -jets for deltino pair production at the Tevatron. The deltino mass is about 97 GeV. (a) gives the distribution when the  $\tau$ -jets come from same sign  $\tau$  leptons. (b) gives the distribution when the  $\tau$ -jets come from opposite sign  $\tau$  leptons.

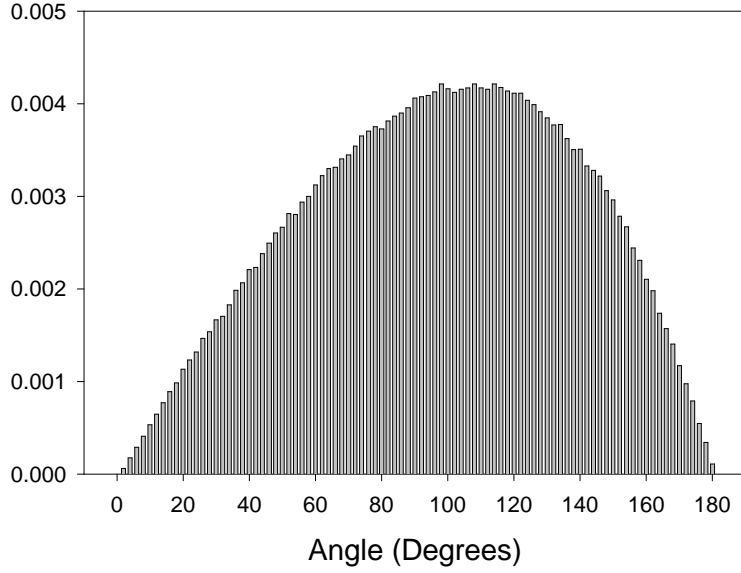


(a)

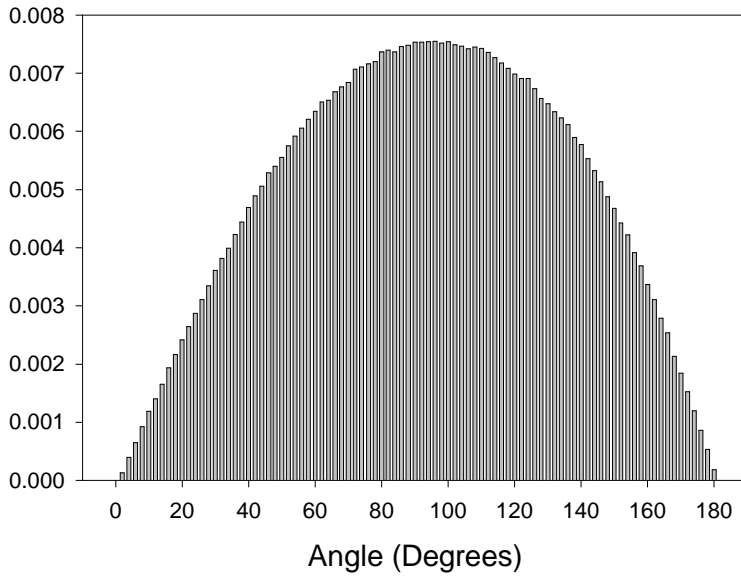


(b)

FIG. 5. Angular distribution between the two most energetic  $\tau$ -jets for EW gaugino production at the Tevatron. The  $\chi_2^0$  mass is 100 GeV. (a) gives the distribution when the  $\tau$ -jets come from same sign  $\tau$  leptons. (b) gives the distribution when the  $\tau$ -jets come from opposite sign  $\tau$  leptons.

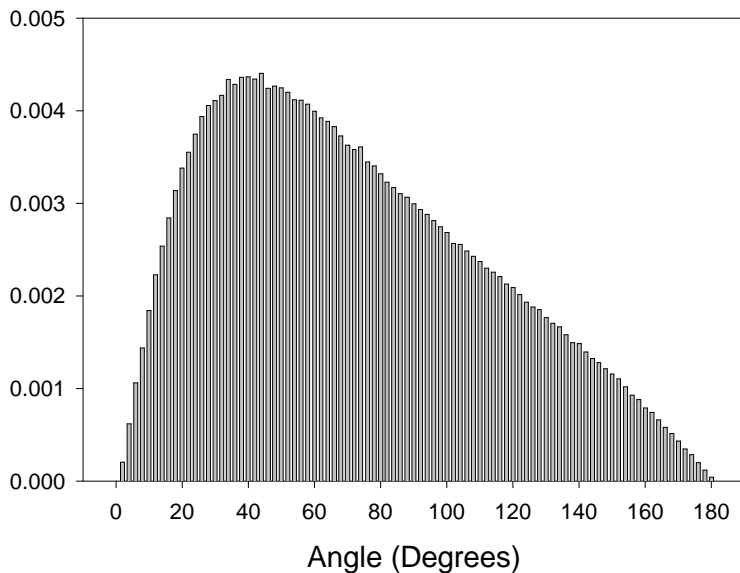


(a)

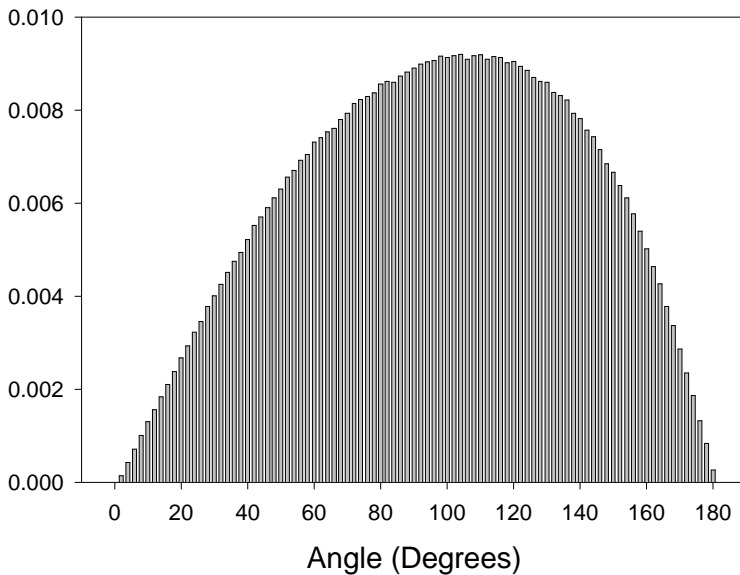


(b)

FIG. 6. Angular distribution between the two most energetic  $\tau$ -jets for EW gaugino production at the Tevatron. The mass of  $\chi_2^0$  is about 150 GeV. (a) gives the distribution when the  $\tau$ -jets come from same sign  $\tau$  leptons. (b) gives the distribution when the  $\tau$ -jets come from opposite sign  $\tau$  leptons.

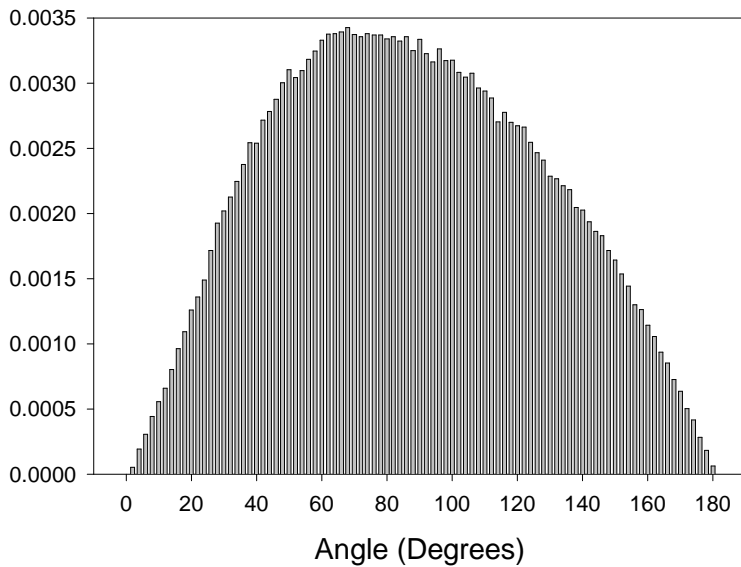


(a)

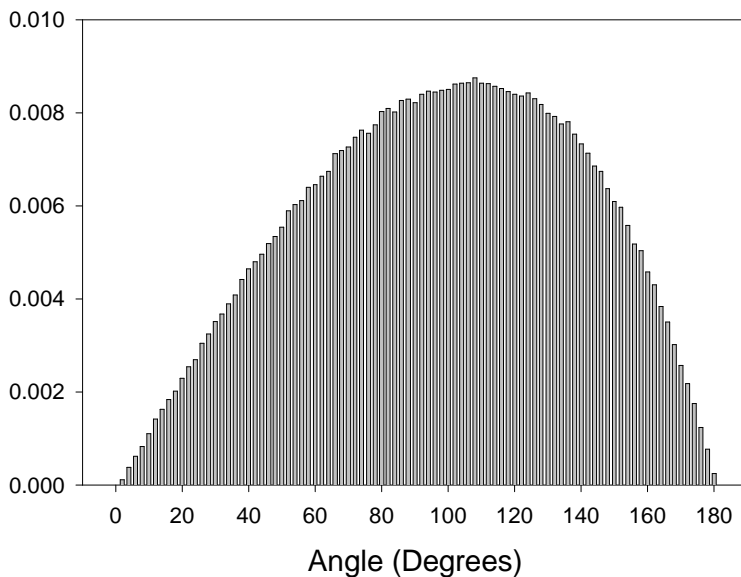


(b)

FIG. 7. Angular distribution between the two most energetic  $\tau$ -jets for combined SUSY pair production at the Tevatron. The messenger scale deltino mass is 90 GeV. The other parameters are  $\tan\beta = 15$ ,  $n = 2$  and  $M/\Lambda = 3$ . (a) gives the distribution when the  $\tau$ -jets come from same sign  $\tau$  leptons. (b) gives the distribution when the  $\tau$ -jets come from opposite sign  $\tau$  leptons.

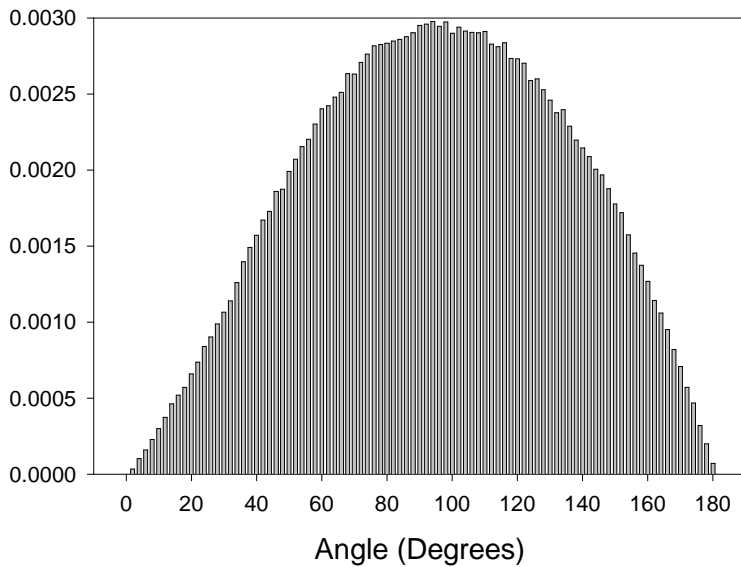


(a)

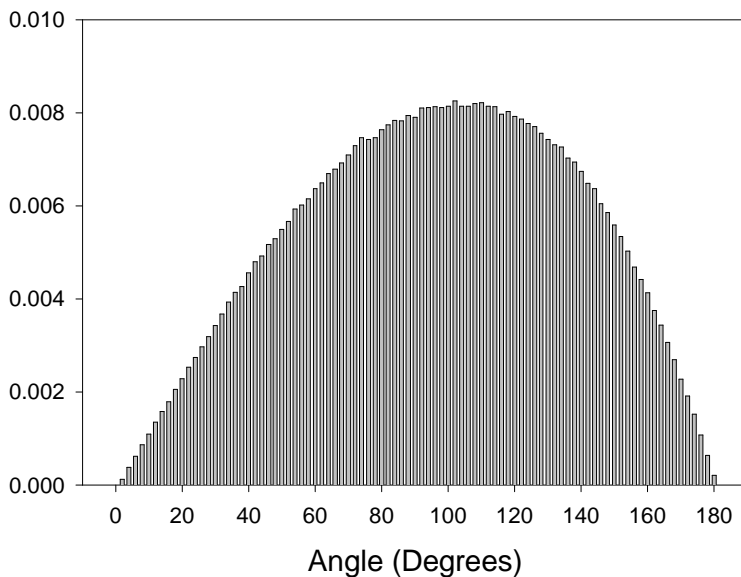


(b)

FIG. 8. Angular distribution between the two most energetic  $\tau$ -jets for combined SUSY production at the Tevatron. The messenger scale deltino mass is 120 GeV. The other parameters are  $\tan \beta = 15$ ,  $n = 2$  and  $M/\Lambda = 3$ . (a) gives the distribution when the  $\tau$ -jets come from same sign  $\tau$  leptons. (b) gives the distribution when the  $\tau$ -jets come from opposite sign  $\tau$  leptons.



(a)



(b)

FIG. 9. Angular distribution between the two most energetic  $\tau$ -jets for combined SUSY production at the Tevatron. The messenger scale deltilino mass is 150 GeV. The other parameters are  $\tan \beta = 15$ ,  $n = 2$  and  $M/\Lambda = 3$ . (a) gives the distribution when the  $\tau$ -jets come from same sign  $\tau$  leptons. (b) gives the distribution when the  $\tau$ -jets come from opposite sign  $\tau$  leptons.